Toronto Metropolitan University

AER606 Component Design and Material Selection

A Study of Systemic Material Selection Methodology and Failure Analysis Theories to Component-Level Designs

Final Report

Authors: Aman Gilani

Abstract

The objective of this design project was to apply systematic material selection methodology and failure analysis theories to component-level design. The purpose of this design project was to design and analysis of a functional and safe aircraft jack that can be used to elevate a low wing, light weight private aircraft such as, Cessna 400 series and Piper Seneca for its repair and maintenance work. Several existing jacks were examined to clearly understand the purpose of different jack types and their application in the industry. For the design task, the aircraft jack's dimensions, load constrains, and mechanisms were referenced from similar existing products particularly the Tripod type aircraft jack. The designed jack is based on a tripod type jack as they are proven to be more stable, durable, and accessible than axel, bipod, or quadruped. The design parameters such as, ultimate loading, height and size of the jack were established from the chosen aircraft, the Cessna 400 Series. The material selection was performed based on important constrains such as cost, weight, manufacturability, and the materials mechanical properties. For the selected material and the given ultimate loadings, a load and stress analysis are conducted for the entire system using the methods of finite elements. Forces calculated for each leg is then used to carryout the buckling analysis to check if the system fails under the ultimate loadings. After the design of the jack is finalized a fracture and a failure analysis is conducted for the structure under the ultimate loadings. For the fracture analysis, the critical crack depth and width are calculated. For the failure analysis, the maximum-distortion-energy theory is used to predict the failure of the structure for the selected materials. The calculated effective stress is then compared to the yield strength to check if the system fails under yielding. The S-N diagram is developed for the selected material and a constant life fatigue analysis is completed based on the goodman line to determine the design limits. The fatigue analysis is conducted based on the ultimate cyclic loading calculated. In the end a section is dedicated towards discussing the manufacturing processes for each component that increases their mechanical properties.

Table of Contents

List of Figures

List of Tables

Introduction

The primary objective of this design project is to design a functional, safe, and economical solution that can elevate a low wing, light weight private aircraft for its repair and maintenance work. During the design and analysis process for this project, various methods of component design and material selection were considered and incorporated to successfully design a strong and an economical aircraft jack. The jack is designed for routine maintenance work on landing gears, wings, and fuselage for a private aircraft such as Cessna 400 series. Currently there are quite a few types of aircraft jack used in the industry, amongst them, tripod and axel jacks are the most common as they provide more stability and accessibility while using. For this project a tripod type aircraft jack is designed as it compliments the loading and height requirements for the chosen aircraft and is more suitable for small maintenance work.

To successfully design a tripod aircraft jack major design constrains indicate the jack to be light weight, portable and sturdy to avoid any lateral movement while in operation. The jack is designed for a low wing, light weight aircraft and is intended be able to lift a weight of 2 US Tons(4000 lbs) without any significant deformations. As there are a large variety of aircraft maintenance and repair work, all with different loadings and ground clearances, the tripod jack is also designed to be height adjustable. For a full body maintenance of a lightweight aircraft, more than one jack can be used to support the weight of the aircraft.

The jack is designed to withstand the critical loading with a safety factor of 1.5 to support the aircraft and ensure no deformations and buckling occur during the life cycle of the jack. When using a single jack for local maintenance or more than one jack for a full body maintenance, the strength of the jack is designed such that it can withstand the maximum empty weight of the aircraft without any fracture or yielding. The tripod jack has a collapsed height of 23 inches with mechanical extension up to 12 inches and a hydraulic extension up to 11 inches. This was a design decision that facilitates the service of the jack to low-wing and high wing aircrafts. With these dimensional and loading constrains, an iterative design process was adopted to build an optimal, light weight and economical tripod aircraft jack.

Review of Existing Design

There are four main types of aircraft jacks used in the industry to raise the aircraft for maintenance and repair works. The Bi-pod jack, Quadruped jack, Tripod jack and the Axle jack are designed for vertical lifting, arc lifting or both vertical and lateral raise. As the names suggest these jacks have different shapes which dictates their stability when in operation.

The Bi-pod jack is designed for arc lifting, it comprises of a hydraulic system which is supported by two fixed rods and one adjustable rod. As seen in the figure, the fixed rods and the adjustable rod provide sturdy support on three sides only making the jack less stable. These rods support the vertical loading is usually tilted through a small angle. The adjustable rod is then used to steady the jack as they move towards the vertical position during an arc lift. The jacking point moves laterally as the aircraft is raised because the aircraft pivots about the wheels of the other undercarriage units.

Figure 1: General Shape of a Bi-pod Aircraft Jack.

The Quadruped jack comprises of a hydraulic system which is supported by two fixed rods and two adjustable rods. This jack has similar advantages to the bipod jack and makes it more stable by adding an additional adjustable rod to it. It also forms the legs into a trestle, which can be rigidly locked when the jack is supporting an aircraft. This jack can be used for an arc lift in a similar manner to the bipod jack.

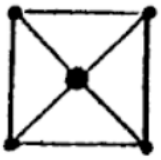

Figure 2: General Shape of a Quadruped Aircraft Jack.

An axle jack is a portable, self-contained hydraulic jack. The lift consists of three rams as well as an outer cylinder. The fluid reservoir is a rectangular tank welded to the base. Axle aircraft jacks are used for aircraft maintenance involving tire repair and replacement, brake

service repair and other maintenance procedures when lifting the nose and/or main landing gear is necessary. Axle jacks are placed directly on or under aircraft landing gear.

Figure 3: Example of an Axle Aircraft Jack.

A tripod jack is a portable, self-contained hydraulic jack. This type of aircraft jack consists of three core parts: a tubular steel tripod structure with caster wheels, a hydraulic cylinder, and a hydraulic pump assembly. Tripod jacks are used for routine maintenance on both the nose and fuselage of the aircraft, specifically they are used for raising the nose, wing or tail of an aircraft and is used by manually operating the hydraulic pump to raise the cylinder and ram. When used in sufficient numbers and placed at the required jacking points, tripod jacks can lift the entire aircraft off the deck.

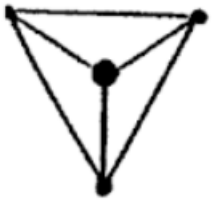

Figure 4: General Shape of a Tripod Aircraft Jack.

Design Parameters

Before doing the material selection and the stress analysis for the aircraft jack, it is important to identify and validate some design parameters based on the given objectives and constrains. The most important factor while designing an aircraft jack in this project, is its accessibility and cost efficiency. Therefore, it is essential to minimize the design weight and yet maintain the aircrafts jack's structural integrity by maximizing the jack's strength and stiffness. The secondary objective for this task is to find a cost-efficient solution to deliver the aircraft jack as an affordable – available to all, device. At the end of this report a section is dedicated towards the manufacturability of the designed aircraft jack. It will discuss and compare different manufacturing processes for each component and how the performance of the jack is maximized. Different manufacturing processes contribute variably towards the component's manufacturing and production costs.

The aircraft jack, for this project, is specifically designed for low wing, light weight aircrafts such as Cessna 400 series aircrafts, Piper Seneca, and Beechcraft Bonanza. This establishes a height constrain for the jack, such that it is able to raise the aircraft for maintenance and repair purposes. The height parameter for this design is decided such that the tripod jack has a collapsed height of 23 inches with mechanical extension up to 12 inches. In order to make the aircraft even more assessable for light weight, high wing aircrafts, a hydraulic extension up to 11 inches can be included due to the increased height constrain for a high wing aircraft.

During the life cycle of the aircraft jack, it is required to lift different aircraft types and several aircraft components. This establishes a limitation for the jack in terms of variable loadings applied during its operational life. For this design process, the loading was defined by keeping in mind the weight of various aircraft components lifted by the jack. It was determined that the jack sustains a maximum ultimate loading of 6000 lbs and a minimum ultimate loading of 1500 lbs. Another crucial parameter for the jack to not buckle or crush under such loading is its size and shape. An optimal trade-off between the jack's shape and size is necessary for the jack to be more durable and resist deformations and buckling under the loadings.

The method of iterative approach is selected to design the tripod type aircraft jack with minimal weight and high fatigue and buckling resistance. The choice of material and the jack

shape are two important free variables during the design process. The material selection will determine the strength, stiffness, and the final weight of each component. The shape of the jack will determine if it is able to resist the above-mentioned failure criteria under the applied loadings. Throughout the project, inspiration from existing jack designs, specifically its function, is taken to design an optimal aircraft jack.

There are various design parameters that influence the design of the jack in different styles. Therefore, it is important to evaluate each parameter and determine what factors are more significant than the other. To achieve this, a decision metrics is tabulated in Table 1 that ranks all the design parameters discussed in previous paragraphs. Each parameter is compared with the other to evaluate if they are less important, equally important, or more important than the other. The key for the metrics is – for less important the score is 0, for equally important the score is 5 and for more important the score is 10. It is expected that the product's mechanical properties and its cost will have more influence in the jack's design and material selection, since the primary objective of this project is to design an aircraft jack that can lift a small aircraft.

Table 1: Design Parameter Decision Metrics.

Criteria	Material Cost	Material Weight	Product Strength and Stiffness	Product Manufacturability	Product Accessibility
Material Cost	NA	Equally Important	Equally Important	Less Important	Less Important
Material Weight	Equally Important	NA	More Important	Equally Important	Equally Important
Product Strength and Stiffness	Equally Important	Less Important	NA	Less Important	Less Important
Product Manufacturability	More Important	Equally Important	More Important	NA	Less Important
Product Accessibility	More Important	More Important	More Important	More Important	NA
Total Points	30/40	20/40	35/40	15/40	5/40

As seen in the above table, the product strength and stiffness criteria were scored the highest, followed by material cost, then material weight, then product manufacturability and lastly product accessibility. From this analysis, it can be said that the design and material selection for the aircraft jack is more skewed towards the product's strength and stiffness rather than its weight. Therefore, it is essential to select a material with good mechanical properties and less cost/kg ratio.

Background Concepts

This section is dedicated towards the discussion of the concepts and math applied during the design of this aircraft jack. To begin with, before doing the stress analysis of any component its is important to select an optimal geometry which reduces the likelihood of failure by any means. For the design of the aircraft jack, to start with a basic tripod geometry in figure 4, it is important to design the columns such that the stress distribution is uniform throughout the material in the part. The uniformity can be achieved by tailoring the element shape to the given loading gradient. Incorporating the use of hollow cylinders as columns can be more effective to create a buckling prone geometry. For the tripod jack design, the diameter of the columns can be changed variably along its length to achieve more uniformity. This practice is known as removing the lazy or slightly stressed material and adding fillets to merge different shapes.

The applied loading on the aircraft jack is due to the aircraft component resting on it. This produces an axial loading on the jack. The force on each leg is evaluated by assuming them as a beam element arbitrarily oriented in space. The entire system is treated as a 3D frame as finite element analysis is used to resolve forces and displacements in each leg. To begin with, a global stiffness matrix is derived for the entire system by deriving and then adding the stiffness matrix for each element. Setting the displacements at the joints as 0, the non-zero displacements are solved from the given axial loading. Next, the reaction forces on the joints are calculated by multiplying the global stiffness matrix and the displacement matrix. The detailed calculations are included in the design summary section.

$$[\lambda_{3x3}] = \begin{bmatrix} l & m & n \\ \frac{-m}{D} & \frac{l}{D} & 0 \\ \frac{-l*n}{D} & \frac{-n*m}{D} & D \end{bmatrix}$$

$$[T] = \begin{bmatrix} [\lambda_{3x3}] & [I] & [I] & [I] \\ [I] & [\lambda_{3x3}] & [I] & [I] \\ [I] & [I] & [\lambda_{3x3}] & [I] \\ [I] & [I] & [I] & [\lambda_{3x3}] \end{bmatrix}$$

$$Stiffness\ Matrix\ in\ global\ axis\ system [k] = [T]^T [k'][T],$$

$$where\ [k']\ is\ the\ element\ stiffness\ matrix\ in\ local\ axis\ system.$$

$$solving\ for\ forces, \{F\} = [K]\{d\}, where\ [K]\ is\ the\ global\ stiffness\ matrix.$$

For the stress analysis of the aircraft jack, the columns are required to resist column buckling or column crushing under the applied loading. Comparing the slenderness ratio to the critical slenderness ratio, the critical buckling can be calculated using the J.B Johnson equations for the given loading and geometric constrains. The stress depends on the material's mechanical and geometric properties and on the column's effective length which depends on its end conditions. The critical buckling stress is calculated as,

$$S_{Cr} = \frac{P_{Cr}}{A} = S_y - \frac{S_y^2}{4 * \pi^2 * E}\left(\frac{L_e}{\rho}\right)^2$$

The primary objecting of any design process is to design the component such that it operates safely and reliably within the prescribed lifetime. Therefore, it is important to conduct a failure analysis to identify potential failure modes based on the applied load and operational environment. Fatigue, buckling and fracture due to crushing are crucial modes of failure concerned with the design of the aircraft jack. Treating the columns as a thick plate, the critical crack size can be determined, above which, if a crack forms in the column it will fail due to brittle fracture.

$$a_{Cr} = \left[\frac{K_{Ic} * \sqrt{0.39 - 0.053\left(\frac{\sigma_g}{S_y}\right)^2}}{\sigma_g}\right]^2$$

For this project, the failure for the aircraft jack can be predicted using the maximum distortion energy theory developed for ductile materials. The basic idea is that if the combination of principal stress gets too large, the material will fail. The equivalent (Von Mises) effective stress is defined as the uniaxial compressive stress that would create the same distortion energy as is created by the actual combination of applied stress. For the component to not fail, the effective stress should be less than the yield stress of the material.

$$S_y^2 \geq \sigma_1^2 + \sigma_2^2 - \sigma_1 * \sigma_2$$

Another important mode of failure for the aircraft jack is fatigue. Fatigue fracture occurs when the component is subjected to repeated or cyclic stress loading. The fracture occurs at stress levels below the material's yield or ultimate strength. Therefore, it is important to select an optimal material and its manufacturing process to avoid cracks during the parts life

cycle. For the aircraft jack's fatigue analysis, it is considered that a varying load is imposed on a constant static loading. Under the given loading and above-mentioned type of fatigue, the endurance limit, the S-N curve, and the component's life cycle are determined in the design summary section.

$$@10^3 cycle,\ S'_f = 0.75 * S_u$$

$$@10^6 cycle,\ S_n = 0.5 * S_u * C_L * C_G * C_S * C_T * C_R$$

Design Summary

Overall summary

The flow chart below represents the process that was adopted for the component design of this project. The load on the aircraft jack is established from the realistic operating load, that is, from the aircraft/aircraft component resting on the jack. For this project, a low wing, light weight aircraft such as Cessna 400 and a Piper Seneca was selected for the load analysis. The applied load was determined from the basic empty weight of these aircrafts, which is 4000 lbs. With a design safety of factor of 1.5, the stress and failure analysis were conducted on the ultimate loading of 6000 lbs.

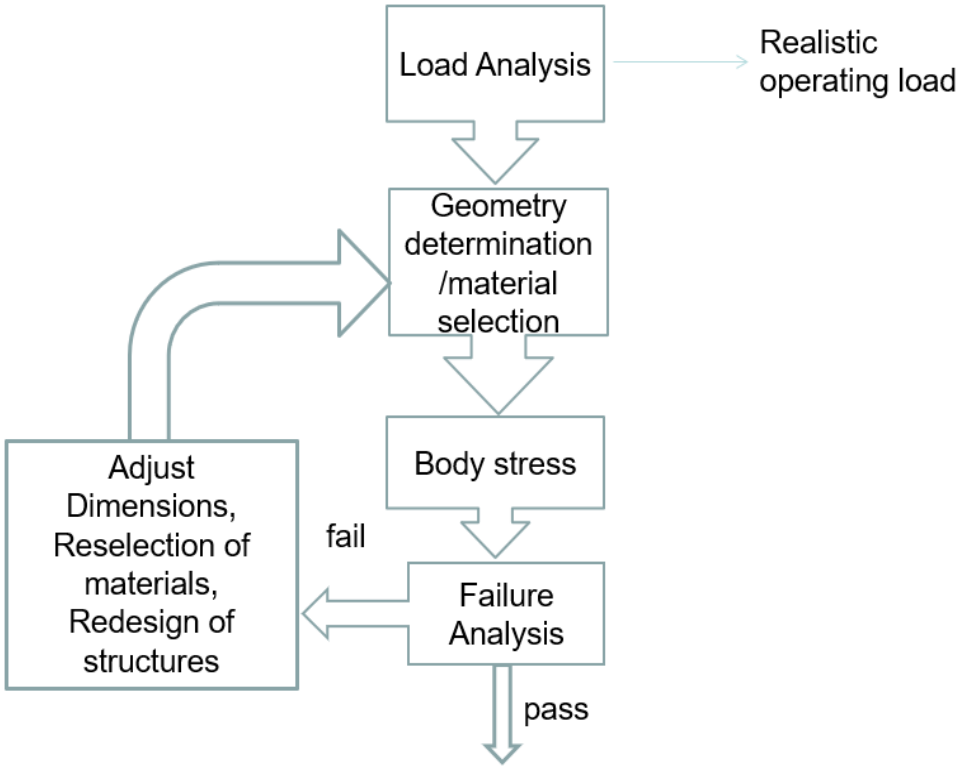

Figure 5: Component Design Process Flow Chart.

The next step in the process is geometry determination. The basic geometry of the jack for this project was inspired from an existing design of a tripod aircraft jack. Different types of jacks were considered for the basic design, which are discussed in the review of existing design section. A tripod type jack was selected because of its portability, stability, and diversity of applications during maintenance. The basic geometry was developed ensuring that the stress distribution is uniform throughout the component. The design theories and models used for the geometry determination are discussed in the background concepts section.

The material selection for the aircraft jack is done based on its functions and constrains. The function of the jack is to safely raise the aircraft like a column under an applied compressive load. As discussed in the design parameters section, the jack is constrained to not buckle or crush under the applied loading. The height of the jack is a fixed variable. The objective of the material selection analysis is to achieve low production costs and light weight. The objective is more skewed towards low costs than light weight as determined by the design metrics(Table 1). A detailed material selection analysis for the given constrains and objective is discussed in the next section.

The jack is treated as a 3D frame with each rod as a beam element. The load analysis on each leg of the tripod jack is done using the FEM analysis. The calculations are included in the stress analysis section and the MATLAB code is included in the appendix section. After doing the load analysis, a buckling analysis is performed using the J.B Johnson equations as discussed in the background concepts section. Based on the applied loadings, the maximum distortion energy theory was used to predict failure of the system. A fatigue analysis is also conducted in the end to determine the endurance limit and the S-N curve for the material selected. The goodman diagram is also established to check if the system fails under fatigue before yielding.

Material Selection

The material selection for the aircraft jack is done based on the function and objectives tabulated in table 2 and the material indices developed from the given constrains.

Table 2: Material Selection for the Aircraft Jack.

Function	Column under Compressive load.
Constrain	1. Must not Fail by Crushing 2. Must not Fail by Buckling 3. Fixed Height 'h' and Fixed Loading 'F'
Objective	Minimize Cost
Free Variables	Diameter 'D' and Material Selection

The material indices are developed to select a material with high strength and high stiffness and minimize cost of the component.

For the column to not crush and minimize cost, $\sigma_c \geq \frac{F*h*\rho*C_m}{C_1} \Longrightarrow C_1 = F * h * \left(\frac{\rho*C_m}{\sigma_c}\right)$

Material Index, $(M_1) = \frac{\rho*C_m}{\sigma_c} = \frac{C_{v,R}}{\sigma_c}$

For the column to not buckle and minimize cost, $\sqrt{F} \leq \frac{C_2^2}{h^2*\rho^2*C_m^2} * \frac{\pi*E}{h^2*4} \Longrightarrow C_2 = 2 * \sqrt{\frac{F*h^4}{\pi}} * \left(\frac{\rho*C_m}{\sqrt{E}}\right)$

Material Index, $(M_2) = \frac{\rho*C_m}{\sqrt{E}} = \frac{C_{v,R}}{\sigma_c}$

To minimize the cost and maximize the stiffness and strength of the material the material indices $\frac{1}{M_1}$ and $\frac{1}{M_2}$ should be maximized. For the developed indices the requirement is to select a material with modulus of elasticity E > 70 GPa, density ρ < 10 Mg/m^3 and strength σ_f > 100 MPa.

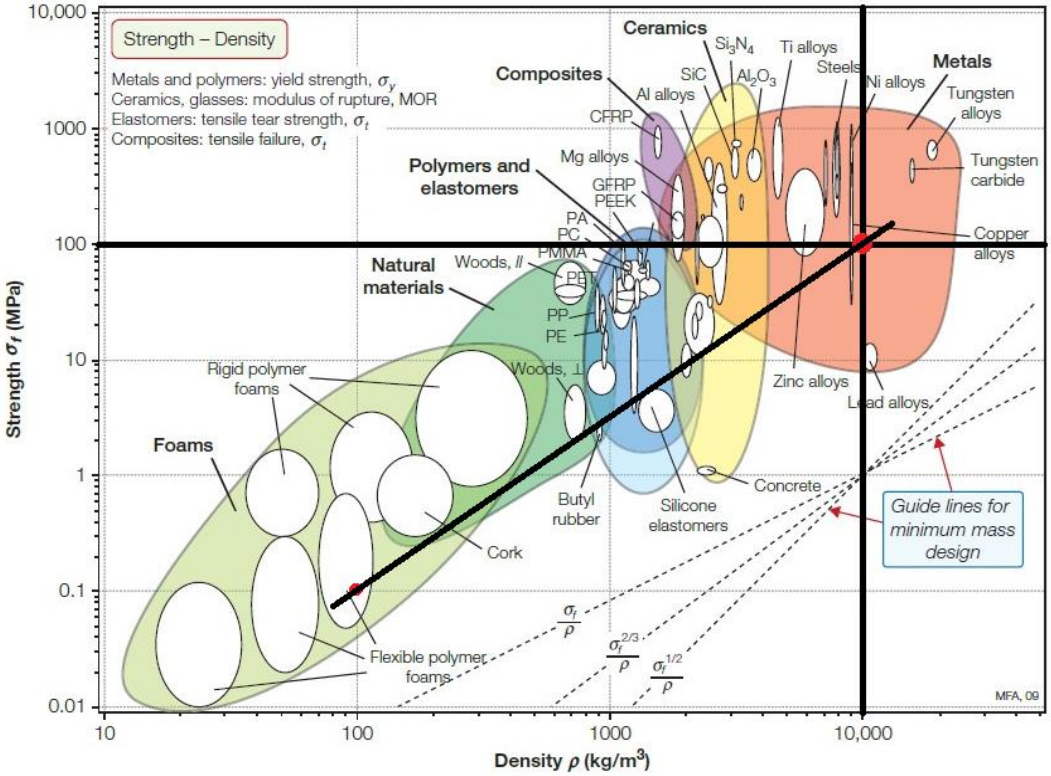

Figure 6: Strength Vs. Density Chart.

From the above strength, density and modulus requirements, the ratios $\frac{1}{M_1}$ and $\frac{1}{M_2}$ are maximized such that $\frac{\sigma_c}{\rho} > 0.01$ and $\frac{\sqrt{E}}{\rho} > 0.0008$.

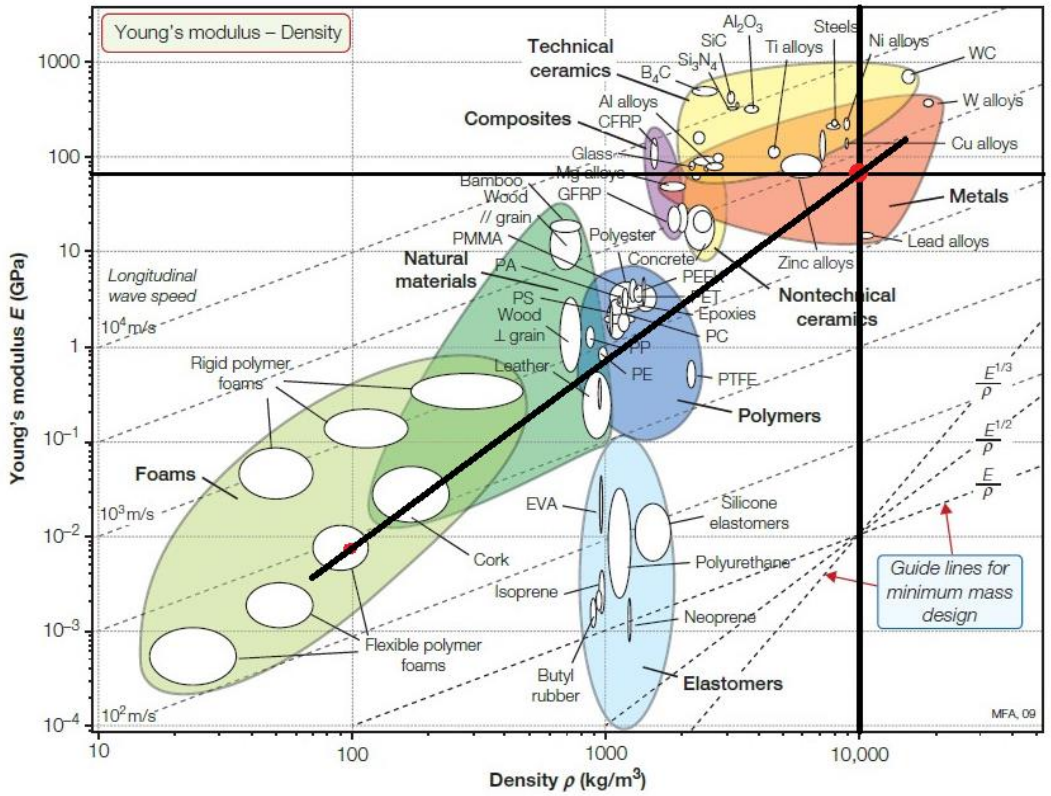

Figure 7: Young's Modulus Vs. Density Chart.

Using the strength-density and modulus-density graphs above the following materials are selected and compared on the basis of their cost per unit Kg. The method of min-max problem is used to select an optimal material.

$$C_1 = F * h * \left(\frac{\rho * C_m}{\sigma_c}\right), where\ F = 2300\ lbs\ and\ h = 25\ in.$$

$$C_2 = 2 * \sqrt{\frac{F * h^4}{\pi}} * \left(\frac{\rho * C_m}{\sqrt{E}}\right), where\ F = 2300\ lbs\ and\ h = 25\ in.$$

$$\bar{C} = \max(C_2\ and\ C_2)$$

Table 3: Material Selection to Minimize Cost.

Materials	Density, ρ (Mg/m^3)	Modulus of Elasticity, E (GPa)	Cost ($/Kg)	Compressive Strength, σ_c (MPa)	C_1	C_2	$\bar{C}$
Steel	7.7	207	0.75	250	0.15	0.58	0.58
Aluminium	2.8	72	1.6	120	0.25	0.77	0.77
Stainless Steal	7.7	190	7	170	2.1	5.7	5.7
Titanium	4.4	114	25	1000	0.7	15	15

From the above table, a steel alloy is chosen as an ideal material that maximizes the strength and stiffness of the material and at the same time minimizes its cost. The steel alloy has a higher density of 7.7 Mg/m^3 as compared to aluminium and titanium alloys in the table. This will result in a heavier design for the aircraft jack. Since it is more important to minimize costs for the material, having high weight is one of the trade-offs of this material selection. Since the C_2 values are higher C_1 for each material, it can be said that the material selection is skewed more towards the stiffness of the material as the applied compressive loading is lesser than the materials compressive strength.

$$Coupling\ Equation: M_2 = M_1 * \frac{1}{2}\sqrt{\frac{F * \pi}{h^2}} = M_2 = M_1 * 141.2$$

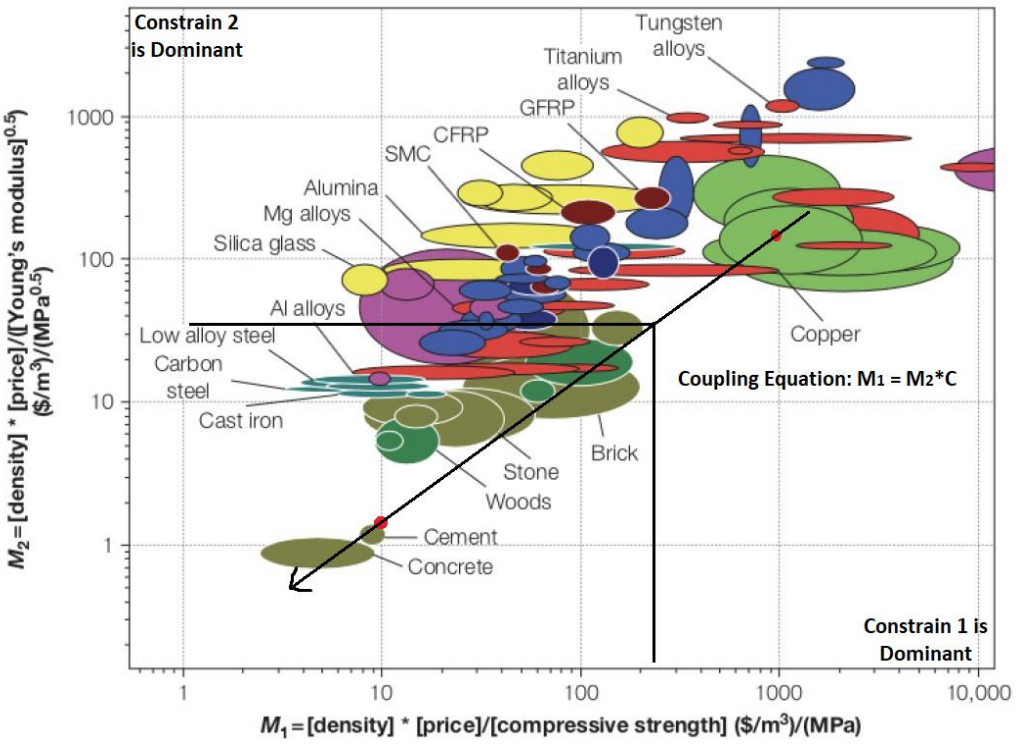

Figure 8: Index M_2 Vs. M_1.

The above graph compares the two material indices by plotting the coupling equation to verify the material selection done above. For steal alloys and aluminium alloys, the buckling constrain(index M_2) is more dominant than the other as expected from the min-max analysis. This implies that the aircraft jack is more likely to fail by buckling than crushing. Even though titanium has excellent mechanical properties, for the aircraft jack design, it is not a good choice of material due to its high cost per unit kg ratio.

Stress Analysis

Iteration 1

The first iteration of the aircraft jack design is adopted from the basic tripod shaped jack currently used in the industry. The design includes a main leg, three supporting legs and a base plate to spread the area of contact with the ground. The figure below illustrates the rough sketch of how the jack would look like. Before doing the stress, and buckling analysis, the known factors include the jack's material, a steel alloy, and the minimum and maximum loadings from the aircraft resting on the jack. The loading is applied on node 5 in the figure below.

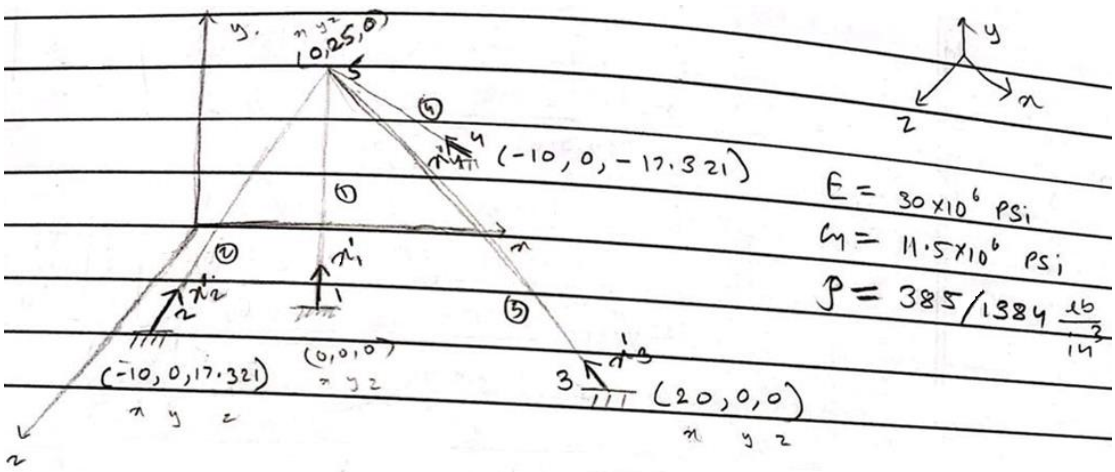

Figure 9: Basic Design of the Aircraft Jack.

To carry out the load analysis for each leg of the jack, the legs are considered as a beam element and the overall structure as a 3D Frame. Then the methods of finite elements are used to develop a stiffness matrix in order to solve for the forces and moments in each leg/beam element. The formulas discussed in the background concepts section are used to carry out the load analysis. The final stiffness matrix was a 30x30 matrix which is multiplied by the displacement matrix to find the forces and moments. Note that nodes 1, 2, 3, and 4 are considered as fully fixed as the legs are fully welded to the base plate. Since the matrix size is so large all the calculations are carried out in MATLAB. The MATLAB code file using the maximum ultimate loading of 6000 lbs is included in the appendix section. To find the minimum loading the forces on node 5 are changed to 1500 lbs. The final maximum and minimum forces on node 5 were calculated to be 2300 lbs and 1000 lbs respectively. The buckling analysis is conducted based on this maximum loading for the main leg. The fatigue analysis is conducted considering the minimum and maximum loading as a cyclic load.

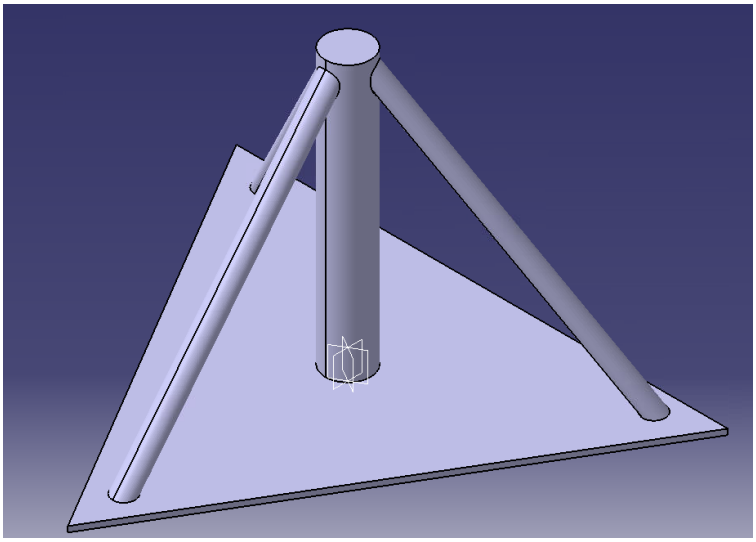

Figure 10: CAD Model - First Iteration.

The engineering drawing for the CAD model is included in the appendix section. The two figures below, figure 10 and 11, illustrates the static structural analysis results from ANSYS. Figure 10 shows the total deformation of the structure designed for the first iteration. The maximum deformation calculated is 0.00032 inches. This is verified from the calculations done with FEM.

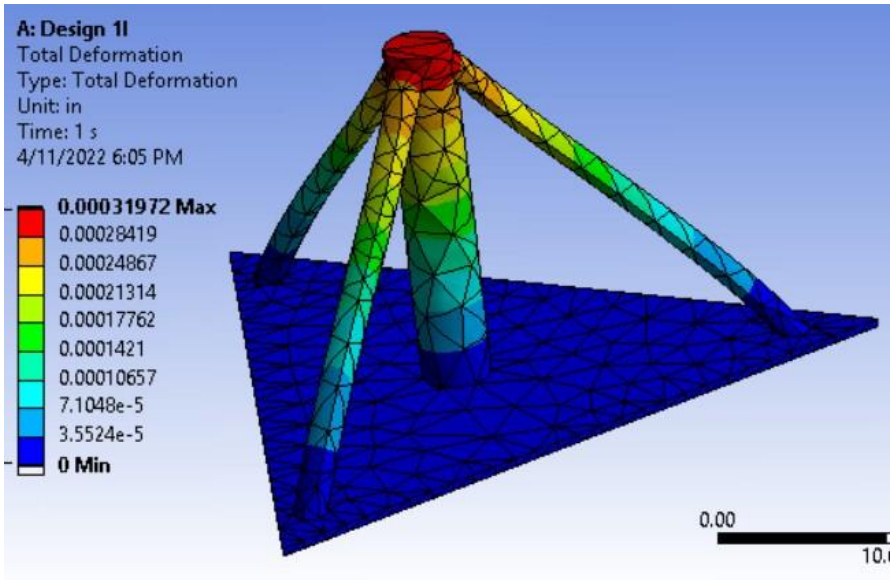

Figure 11: ANSYS Simulation for Total Deformation - First Iteration.

The second figure, figure 11, illustrated the equivalent Von-Mises stress of the structure. The maximum stress is calculated to be 591.29 Psi at the joints as seen in the figure. The maximum stress calculated using the finite element methods was 550 Psi. The slight difference in the two is due to the difference in methods used to calculate the stress.

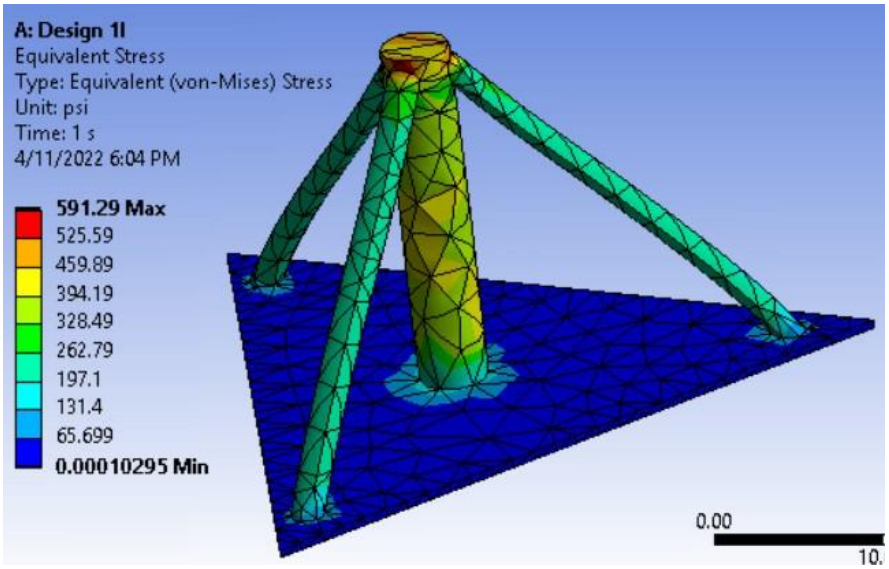

Figure 12: ANSYS Simulation for Von-Mises Stress - First Iteration.

Now that the loadings are resolved for each leg, the buckling analysis is performed for each leg to determine if the design fails under buckling. This analysis will also determine the critical stress for the given dimensions and loading. For the vertical column(Main leg) the axial loading was calculated to be 2300 lbs including the 1.5 safety of factor. The actual load is 1533 lbs. The buckling calculations for the three supporting legs are presented in the appendix section.

$$\rho = \sqrt{\frac{I}{A}} = 19.2 \; and \; L_e = 50$$

$$SR = \frac{L_e}{\rho} = 2.6$$

$$SR_{Cr} = \sqrt{\frac{2 * \pi^2 * E}{S_y}} = 99$$

$$S_{Cr} = S_y - \frac{S_y^2}{4 * \pi^2 * E} * \left(\frac{L_e}{\rho}\right)^2 = 220 \; Psi$$

$$P_{Cr} = S_{Cr} * A = 2765 \; lbs$$

$$Actual \; SF = \frac{P_{Cr}}{P_{actual}} = 1.8$$

Iteration 2

As seen from the above buckling and stress analysis, the structure will not buckle or crush under the applied ultimate loadings. Therefore, for the second iteration the focus was to reduce the weight of the structure. This was achieved by reducing the slightly stressed components and adding fillets to sharp corners. The radius of the main leg was increased

from 2 to 3 inches. The radius for the three supporting legs were increased from 1 to 1.5 inches. The area reduction for the base plate was achieved by reducing the slightly stressed areas and adding fillets to sharp corners for an even stress distribution. The engineering drawing for the CAD model is included in the appendix section.

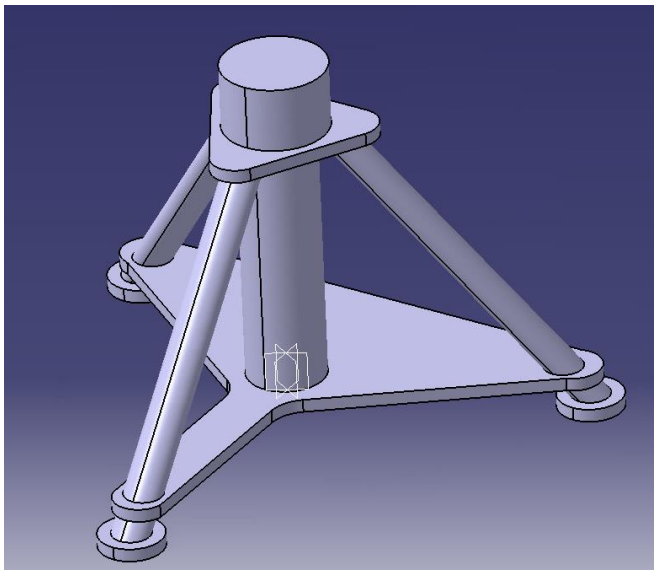

Figure 13: CAD Model - Iteration 2.

The new structure was solved again using the ANSYS static structural tool. The maximum total deformation was calculated to be 0.0007. As compared to the first iteration structure the displacement is doubled as expected due to the increased radius for the four legs.

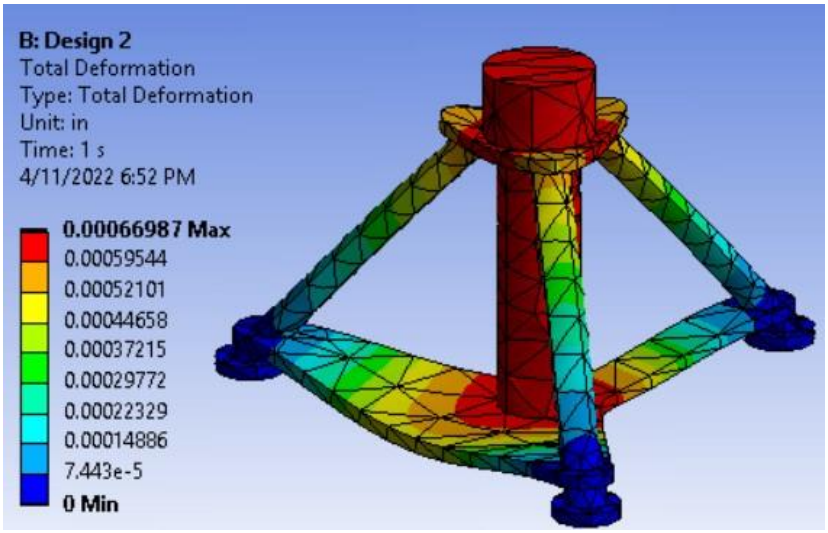

Figure 14: ANSYS Simulation for Total Deformation - Second Iteration.

The figure below, figure 13, illustrates the equivalent Von-Mises stress for the second structure. The maximum stress was calculated to be 667 Psi at the joints. The stress level

also increased slight from the first structure due to the area reduction. This maximum stress is still lower than the

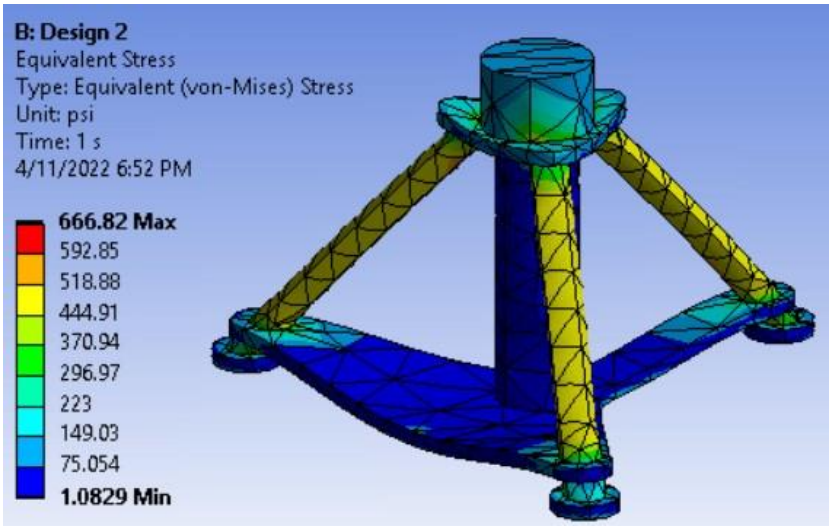

Figure 15: ANSYS Simulation for Von-Mises Stress - Second Iteration.

Fracture and Failure Analysis

This section will discuss the fracture and failure modes for the designed aircraft jack. For every design it is essential to study the impact of the loads on the structure to determine the components life cycle. In this report, the method of max distortion energy theory is used to develop the failure modes since it is more accurate than the more conservative max shear stress theory. In the end a goodman estimation analysis is conducted to check the dominant failure mode for the part between fatigue and yielding. The table below compares the selected materials strength properties. Since the ideal material selected for the aircraft jack was steel alloy, all the following calculations are based on its respective strength properties.

Table 4: Material Strength Properties.

Materials	**Ultimate Strength, S_u (KPsi)**	**Yield Strength, S_y (KPsi)**	**K_{Ic} (KPsi $in^{0.5}$)**
Steel	260	217	52
Aluminium	78	70	27
Stainless Steal	220	190	70
Titanium	130	120	65

A sharp crack can suddenly lead to component failure because of the sudden increase in stress concentration around the crack. The first step in such failure mode is crack generation followed by crack propagation and then failure. Such failure can occur at lower stresses than the components yield strength. The critical crack size due to stress levels that are 75% of the

yield strength is predicted for this analysis. If the crack size increases more than the calculated value below the component fails due to crack propagation.

$$Crack\ Depth, a_{Cr} = \left[\frac{K_{Ic}\sqrt{0.39 - 0.053\left({}^{\sigma_y}/_{S_y}\right)^2}}{\sigma_y}\right]^2 = 0.037\ in = 0.9\ mm$$

$$Crack\ Width, 2c = \frac{a_{Cr}}{0.25} = 0.15\ in = 3.8\ mm$$

The Max Distortion Energy Theory is used to predict ductile yielding for the aircraft jack. For the design to be safe, the effective stress calculated must be less than the materials yield strength. the principal stresses are calculated as follows with $\sigma_x = 0, \sigma_y = -185\ KPsi\ and\ \tau_{xy} = 0.$

$$\sigma_y = \frac{F_y}{A} = -185\ KPsi$$

$$\sigma_1, \sigma_2 = \frac{\sigma_x + \sigma_y}{2} \pm \sqrt{\left(\tau_{xy}\right)^2 + \left(\frac{\sigma_x - \sigma_y}{2}\right)^2} = 0\ KPsi, -185\ KPsi$$

$$\sigma_e = \sqrt{\sigma_1^2 + \sigma_2^2 - \sigma_1 * \sigma_2} = 185\ KPsi$$

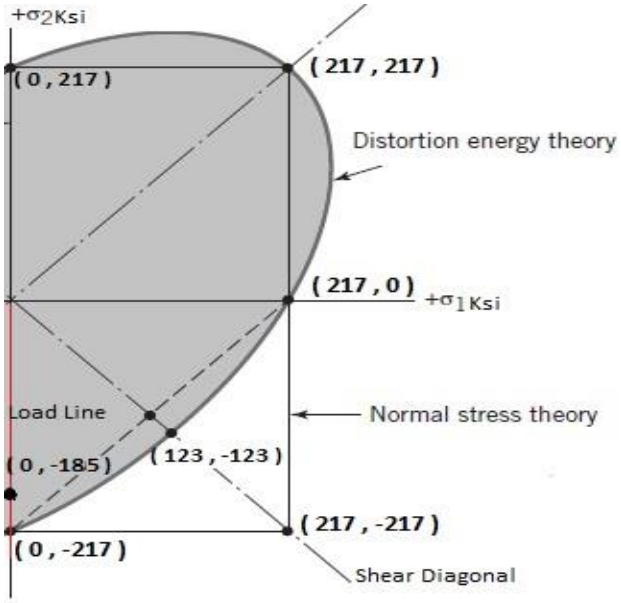

Figure 16: Max-Distortion-Energy Failure Theory.

Comparing the yield strength of steel from table 4 to the above calculated effective stress, $S_y > \sigma_e$. Therefore, we can say that the design will not fail due to ductile yielding. The yield safety factor from the max distortion energy theory is calculated as: $SF = \frac{S_y}{\sigma_e} = 1.17$.

For the life cycle and endurance limit analysis for the selected material, a 90% reliability is assumed with surface factor of 0.9 and gradient factor of 0.8.

$$@10^3 cycle,\ S'_f = 0.75 * S_u = 195\ KPsi$$

$$S'_n = 0.5 * S_u = 130\ KPsi$$

$$@10^6 cycle,\ S_n = S'_n * C_L * C_G * C_S * C_T * C_R = 84\ KPsi$$

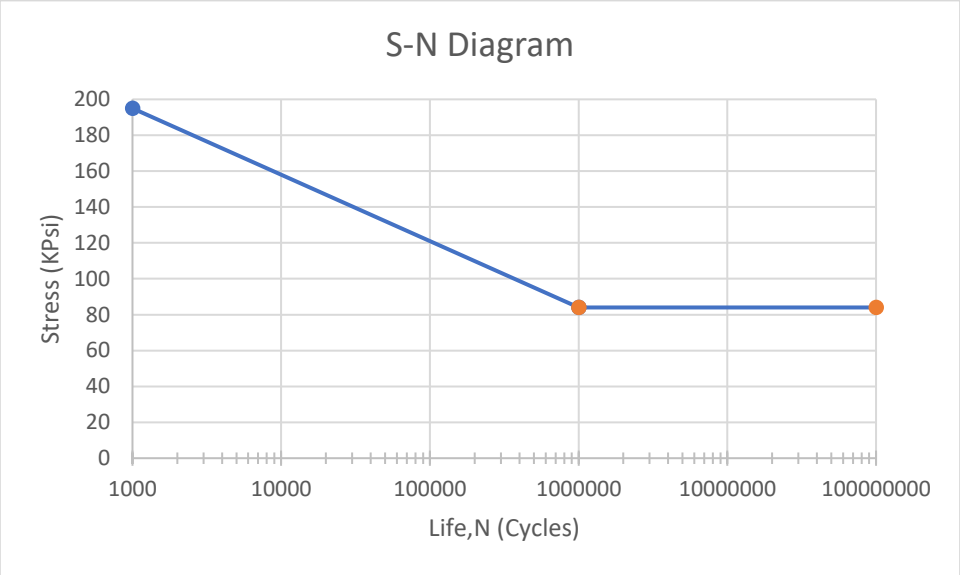

Figure 17: S-N Diagram.

The aircraft jack is considered to have a varying load imposed on a constant static loading. The loading varies between 2300 lbs and 1000 lbs. The maximum value is derived from the maximum weight of the aircraft resting on the jack and the minimum load is derived from the weight of the component of the aircraft such as the wing or the landing gear. This varying loading is an example of cyclic loading which can cause fatigue failure of the component. The goodman estimation is used to check the dominant mode of failure between fatigue and yielding.

$$F_a = \frac{F_{max} - F_{min}}{2} = 650\ lbs$$

$$F_m = \frac{F_{max} + F_{min}}{2} = 1650\ lbs$$

$$\frac{\sigma_a}{\sigma_m} = \frac{13}{33}$$

$$Goodman\ Gradient: \frac{\sigma_a}{S_n} + \frac{\sigma_m}{S_u} = 1$$

$$Yield\ Line: \frac{\sigma_a + \sigma_m}{S_y} = 1$$

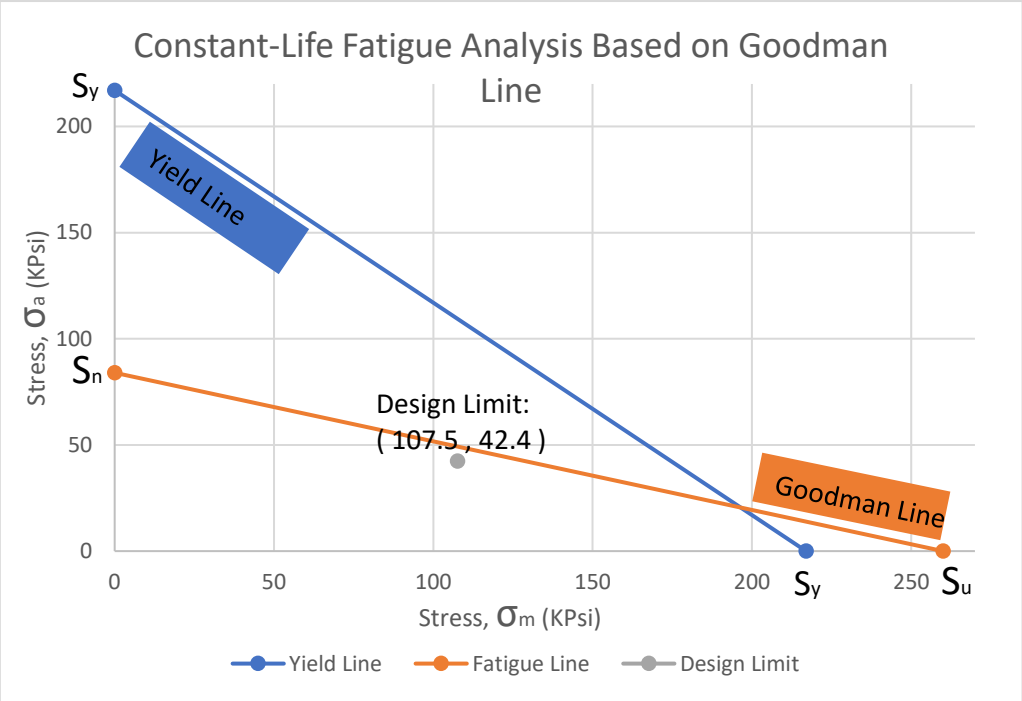

Figure 18: Fatigue Analysis Based on Goodman Line.

The above figure illustrates the fatigue analysis based on the goodman line. The design limits were determined to be $\sigma_a = 107.5$ Kpsi and $\sigma_m = 42.4$ Kpsi. If the loading exceeded the design limit the component is predicted to fail due to fatigue before yielding. Therefore, fatigue is a more dominant failure mode for the designed jack.

In this design, the main leg and the 3 supporting legs are welded to the base plate. In several instances the welded joints have reduced material properties and contain defects. The increase in thermal expansion during welding generates residual stress in the welded joints. This is an area of concern as these locations tend to be critical in terms of deformations, fracture, and fatigue. For this project the residual stress analysis was not performed as it was out of scope for this course. For future design considerations, post-weld treatments can be implemented to relieve residual stresses in the welded joints. Methods like shot peening and cold rolling can be used to achieve this.

Manufacturing Methods

This section will discuss a possible manufacturing method for the designed aircraft jack. The objective is to improve the mechanical properties of the materials used with emphasis on increasing its hardness and removing the internal stress. For the assembly of the aircraft jack, it is necessary to manufacture each component separately. Then joining method such as welding, can be used to join the legs and the plate. The residual stress in the welded joints can be removed using heat treatment methods such as normalizing or tempering. Removing the residual stress decreases the critical failure points in the joints. Tempering also reduces the brittleness of the metal. The jack's legs can be manufactured through cold drawing of the raw material. Then the process of CNC machining of steel can be used to form steel columns(legs) of this aircraft jack. The raw materials can undergo heat treatment, such as hardening, to increase the leg's strength and hardness. To produce thin base plate for the aircraft jack, the raw materials can be melted and casted onto a flat plate die. Then the process of shearing and forming can be used to cut the plate into the desired shape. Similar methods of heat treatment can be used to increase the plates strength and hardness.

Conclusion

The objective of this design project was to apply systematic material selection methodology and failure analysis theories to component-level design. The task was to design a functional and an economic aircraft jack capable of raising a lightweight aircraft for its maintenance and repair purposes. For the initial design of the jack an existing design, a tripod type jack, was considered for its stability and range of application. An iterative approach was adopted to redesign the jack and carry out a comprehensive stress analysis. An optimal material was selected based on the given constrains and objectives and developed material indexes for the aircraft jack. The aim of this material selection was to reduce the cost of each component but at the same time select a material with high strength and stiffness. For the applied maximum and minimum ultimate loadings, a buckling analysis is done to verify that the structure does not fail. The maximum-distortion-energy theory of failure in ductile materials is used to verify if the design fails under yield stress. A 3D model for both iterations are developed in CATIA, and a static structural analysis is done on ANSYS to verify the stress calculations for the finite element analysis. The critical crack size is calculated to determine the maximum depth and width of a crack that can occur before the structure fails due to fracture. The S-N diagram is developed for the chosen material – steel alloy to determine the stress levels at 10^6 and 10^3 life cycles. A final constant life fatigue analysis is conducted based on the goodman line. The design limit suggests that the system will fail due to fatigue stress under the design limits. In the end, different manufacturing methods are discussed for each component. Different methods of increasing the materials mechanical properties and reducing the internal stress are also discussed in this section. Looking at the overall design of the aircraft jack, the jack is designed to sustain the ultimate loadings and the cyclic loadings calculated. The jack will not buckle or yield under the given loadings.

References

1. “Types of aircraft jacks,” *Types of Aircraft Jacks*. [Online]. Available: https://aviamech.blogspot.com/2011/05/types-of-aircraft-jacks.html. [Accessed: 15-Apr-2022].
2. “The 2 most common types of aircraft jacks and when to use which,” *Tronair*. [Online]. Available: https://www.tronair.com/resources/types-of-aircraft-jacks/. [Accessed: 15-Apr-2022].
3. “2 types of hydraulic aircraft jacks: Tripod & Axle,” *FlyTek GSE*, 07-Jul-2021. [Online]. Available: https://flytekgse.com/2019/09/23/types-of-aircraft-jacks/#:~:text=Aircraft%20jacks%20are%20a%20fundamental,by%20far%20the%20most%20common. [Accessed: 15-Apr-2022].
4. “Online materials information resource,” *MatWeb*. [Online]. Available: https://www.matweb.com/index.aspx. [Accessed: 15-Apr-2022].
5. A. A. DeWald, “Residual stress in welding,” *Hill Engineering*, 19-Mar-2021. [Online]. Available: https://hill-engineering.com/residual-stress-measurement/residual-stress-welding/. [Accessed: 15-Apr-2022].
6. “What is residual stress?” *TWI*. [Online]. Available: https://www.twi-global.com/technical-knowledge/faqs/residual-stress. [Accessed: 15-Apr-2022].
7. D. A. R. Y. L. L. LOGAN, “Chapter 5: Frame and Grid Equations.,” in *First course in the finite element method*, S.l.: CENGAGE LEARNING, 2022.
8. B. Tan, “Lecture slides: Week 3,” in *AER 606*.
9. B. Tan, “Lecture slides: Week 5,” in *AER 606*.
10. B. Tan, “Lecture slides: Week 6,” in *AER 606*.
11. B. Tan, “Lecture slides: Week 7,” in *AER 606*.
12. B. Tan, “Lecture slides: Week 8,” in *AER 606*.

Appendix

Table 8.1 Generalized Fatigue Strength Factors for Ductile Materials (*S–N* curves)

a. 10^6-cycle strength (endurance limit)[a]

Bending loads: $S_n = S'_n C_L C_G C_S C_T C_R$

Axial loads: $S_n = S'_n C_L C_G C_S C_T C_R$

Torsional loads: $S_n = S'_n C_L C_G C_S C_T C_R$

where S'_n is the R.R. Moore, endurance limit,[b] and

		Bending	Axial	Torsion
C_L	(load factor)	1.0	1.0	0.58
C_G	(gradient factor): diameter < (0.4 in. or 10 mm)	1.0	0.7 to 0.9	1.0
	(0.4 in. or 10 mm) < diameter < (2 in. or 50 mm)[c]	0.9	0.7 to 0.9	0.9
C_S	(surface factor)	see Figure 8.13		
C_T	(temperature factor)	Values are only for steel		
	$T \leq 840$ °F	1.0	1.0	1.0
	840 °F < T ≤ 1020 °F		1 − (0.0032T − 2.688)	
C_R	(reliability factor):[d]			
	50% reliability	1.000	"	"
	90% "	0.897	"	"
	95% "	0.868	"	"
	99% "	0.814	"	"
	99.9% "	0.753	"	"

b. 10^3-cycle strength[e, f, g]

Bending loads: $S_f = 0.9 S_u C_T$

Axial loads: $S_f = 0.75 S_u C_T$

Torsional loads: $S_f = 0.9 S_{su} C_T$

where S_u is the ultimate tensile strength and S_{su} is the ultimate shear strength.

Figure 19: S-N Curve Calculation Parameters.

Buckling Calculations for the three supporting legs:

$$\rho = \sqrt{\frac{I}{A}} = 21.7 \; and \; L_e = 32.02$$

$$SR = \frac{L_e}{\rho} = 21.7$$

$$SR_{Cr} = \sqrt{\frac{2 * \pi^2 * E}{S_y}} = 99$$

$$S_{Cr} = S_y - \frac{S_y^2}{4 * \pi^2 * E} * \left(\frac{L_e}{\rho}\right)^2 = 198 \; Psi$$

$$P_{Cr} = S_{Cr} * A = 623 \; lbs$$

$$Actual \; SF = \frac{P_{Cr}}{P_{actual}} = 1.78, P_{actual} = 350 \; lbs \; for \; each \; leg.$$

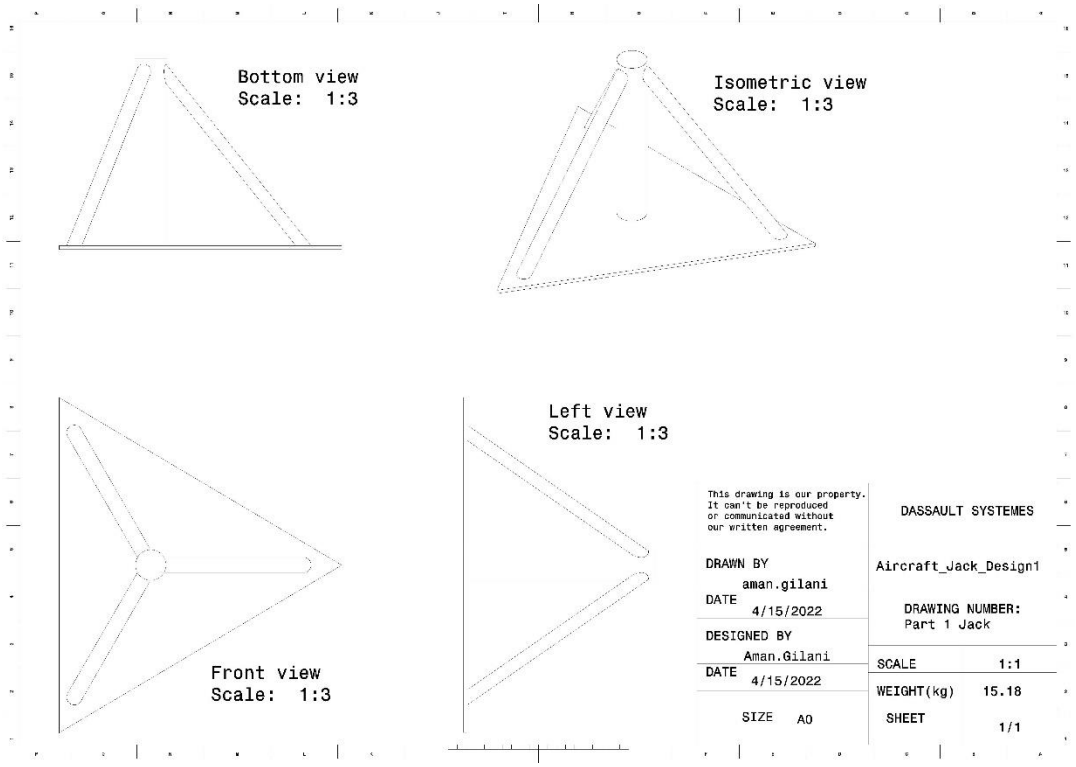

Figure 20: Aircraft Jack, Engineering Drawing - First Iteration.

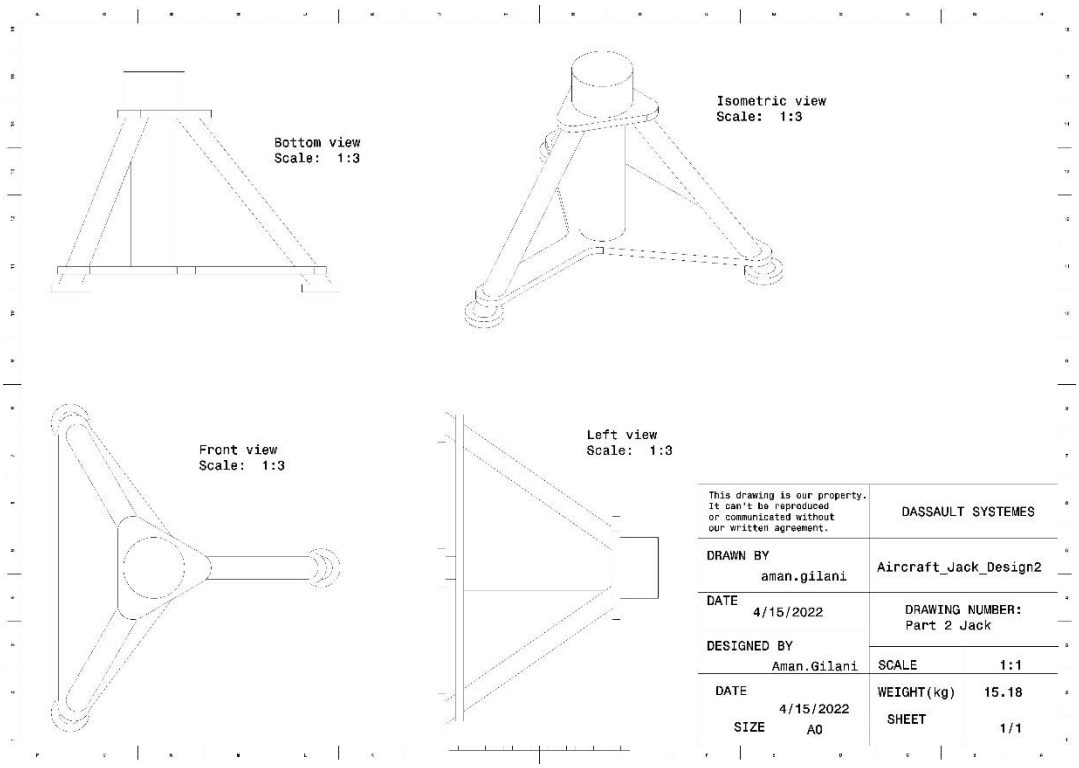

Figure 21: Aircraft Jack, Engineering Drawing - Second Iteration.

AER606 Design Project

Table of Contents

Developed by: Aman Gilani, 500879895

Symbolic Calculations.

```
%{
clc
clear

syms E G A L J I
syms l m n D
syms k T K out

% Local Stiffness Matrix for a Single Element.
k = [(A*E)/L 0 0 0 0 0 -(A*E)/L 0 0 0 0 0;
      %u1
      0 (12*E*I)/L^3 0 0 0 (6*E*I)/L^2 0 -(12*E*I)/L^3 0 0 0 (6*E*I)/
L^2;   %v1
      0 0 (12*E*I)/L^3 0 -(6*E*I)/L^2 0 0 0 -(12*E*I)/L^3 0 -(6*E*I)/
L^2 0; %w1
      0 0 0 G*J/L 0 0 0 0 0 -G*J/L 0 0;
      %phi_1x
      0 0 -(6*E*I)/L^2 0 (4*E*I)/L 0 0 0 (6*E*I)/L^2 0 (2*E*I)/L 0;
      %phi_1y
      0 (6*E*I)/L^2 0 0 0 (4*E*I)/L 0 -(6*E*I)/L^2 0 0 0 (2*E*I)/L;
      %phi_1z
      -(A*E)/L 0 0 0 0 0 (A*E)/L 0 0 0 0 0;
      %u2
      0 -(12*E*I)/L^3 0 0 0 -(6*E*I)/L^2 0 (12*E*I)/L^3 0 0 0 -
(6*E*I)/L^2; %v2
      0 0 -(12*E*I)/L^3 0 (6*E*I)/L^2 0 0 0 (12*E*I)/L^3 0 (6*E*I)/L^2
 0;   %w2
      0 0 0 -G*J/L 0 0 0 0 0 G*J/L 0 0;
      %phi_2x
      0 0 (6*E*I)/L^2 0 (2*E*I)/L 0 0 0 (6*E*I)/L^2 0 (4*E*I)/L 0;
      %phi_2y
      0 (6*E*I)/L^2 0 0 0 (2*E*I)/L 0 -(6*E*I)/L^2 0 0 0 (4*E*I)/L];
      %phi_2z

% Transformation Matrix for a Single Element.
```

```
T = [l m n 0 0 0 0 0 0 0 0 0;
       -m/D l/D 0 0 0 0 0 0 0 0 0 0;
       -(l*n)/D -(m*n)/D D 0 0 0 0 0 0 0 0 0;
       0 0 0 l m n 0 0 0 0 0 0;
       0 0 0 -m/D l/D 0 0 0 0 0 0;
       0 0 0 -(l*n)/D -(m*n)/D D 0 0 0 0 0 0;
       0 0 0 0 0 0 l m n 0 0 0;
       0 0 0 0 0 0 -m/D l/D 0 0 0;
       0 0 0 0 0 0 -(l*n)/D -(m*n)/D D 0 0 0;
       0 0 0 0 0 0 0 0 0 l m n;
       0 0 0 0 0 0 0 0 0 -m/D l/D 0;
       0 0 0 0 0 0 0 0 0 -(l*n)/D -(m*n)/D D];

% Global Stiffness Matrix for a Single Element.
K = T'*k*T;

% Extracting the Non-Zero Terms.
out = K(7:12,7:12)
%}
```

Substituting Values for Element 1.

```
clear
clc

E = 30*10^6;
G = 11.5*10^6;
A = 4*pi;
L = 25;
J = 8*pi;
I = 4639.1;

l = 0;
m = 1;
n = 0;
D = 1;

k_E1 = [(A*E)/L 0 0 0 0 0 -(A*E)/L 0 0 0 0 0;
      %u1
      0 (12*E*I)/L^3 0 0 0 (6*E*I)/L^2 0 -(12*E*I)/L^3 0 0 0 (6*E*I)/
L^2;   %v1
      0 0 (12*E*I)/L^3 0 -(6*E*I)/L^2 0 0 0 -(12*E*I)/L^3 0 -(6*E*I)/
L^2 0; %w1
      0 0 0 G*J/L 0 0 0 0 0 -G*J/L 0 0;
      %phi_1x
      0 0 -(6*E*I)/L^2 0 (4*E*I)/L 0 0 0 (6*E*I)/L^2 0 (2*E*I)/L 0;
      %phi_1y
      0 (6*E*I)/L^2 0 0 0 (4*E*I)/L 0 -(6*E*I)/L^2 0 0 0 (2*E*I)/L;
      %phi_1z
      -(A*E)/L 0 0 0 0 0 (A*E)/L 0 0 0 0 0;
      %u2
      0 -(12*E*I)/L^3 0 0 0 -(6*E*I)/L^2 0 (12*E*I)/L^3 0 0 0 -
(6*E*I)/L^2; %v2
```

```
      0 0 -(12*E*I)/L^3 0 (6*E*I)/L^2 0 0 0 (12*E*I)/L^3 0 (6*E*I)/L^2
 0;   %w2
      0 0 0 -G*J/L 0 0 0 0 0 G*J/L 0 0;
      %phi_2x
      0 0 (6*E*I)/L^2 0 (2*E*I)/L 0 0 0 (6*E*I)/L^2 0 (4*E*I)/L 0;
      %phi_2y
      0 (6*E*I)/L^2 0 0 0 (2*E*I)/L 0 -(6*E*I)/L^2 0 0 0 (4*E*I)/L];
      %phi_2z

T_E1 = [l m n 0 0 0 0 0 0 0 0 0;
       -m/D l/D 0 0 0 0 0 0 0 0 0;
       -(l*n)/D -(m*n)/D D 0 0 0 0 0 0 0 0;
       0 0 0 l m n 0 0 0 0 0 0;
       0 0 0 -m/D l/D 0 0 0 0 0 0;
       0 0 0 -(l*n)/D -(m*n)/D D 0 0 0 0 0;
       0 0 0 0 0 0 l m n 0 0 0;
       0 0 0 0 0 0 -m/D l/D 0 0 0;
       0 0 0 0 0 0 -(l*n)/D -(m*n)/D D 0 0 0;
       0 0 0 0 0 0 0 0 0 l m n;
       0 0 0 0 0 0 0 0 0 -m/D l/D 0;
       0 0 0 0 0 0 0 0 0 -(l*n)/D -(m*n)/D D];

K_E1 = T_E1'*k_E1*T_E1;

out_E1 = K_E1(7:12,7:12);
```

Substituting Values for Element 2.

```
E = 30*10^6;
G = 11.5*10^6;
A = pi;
L = 32.016;
J = pi/2;
I = 1485.250713;

l = 625/2001;
m = 3125/4002;
n = -0.541;
D = 0.841;

k_E2 = [(A*E)/L 0 0 0 0 0 -(A*E)/L 0 0 0 0 0;
      %u1
      0 (12*E*I)/L^3 0 0 0 (6*E*I)/L^2 0 -(12*E*I)/L^3 0 0 0 (6*E*I)/
L^2;   %v1
      0 0 (12*E*I)/L^3 0 -(6*E*I)/L^2 0 0 0 -(12*E*I)/L^3 0 -(6*E*I)/
L^2 0; %w1
      0 0 0 G*J/L 0 0 0 0 0 -G*J/L 0 0;
      %phi_1x
      0 0 -(6*E*I)/L^2 0 (4*E*I)/L 0 0 0 (6*E*I)/L^2 0 (2*E*I)/L 0;
      %phi_1y
      0 (6*E*I)/L^2 0 0 0 (4*E*I)/L 0 -(6*E*I)/L^2 0 0 0 (2*E*I)/L;
      %phi_1z
```

```
      -(A*E)/L 0 0 0 0 0 (A*E)/L 0 0 0 0 0;
      %u2
      0 -(12*E*I)/L^3 0 0 0 -(6*E*I)/L^2 0 (12*E*I)/L^3 0 0 0 -
(6*E*I)/L^2; %v2
      0 0 -(12*E*I)/L^3 0 (6*E*I)/L^2 0 0 0 (12*E*I)/L^3 0 (6*E*I)/L^2
 0;   %w2
      0 0 0 -G*J/L 0 0 0 0 0 G*J/L 0 0;
      %phi_2x
      0 0 (6*E*I)/L^2 0 (2*E*I)/L 0 0 0 (6*E*I)/L^2 0 (4*E*I)/L 0;
      %phi_2y
      0 (6*E*I)/L^2 0 0 0 (2*E*I)/L 0 -(6*E*I)/L^2 0 0 0 (4*E*I)/L];
      %phi_2z

T_E2 = [l m n 0 0 0 0 0 0 0 0 0;
       -m/D l/D 0 0 0 0 0 0 0 0 0;
       -(l*n)/D -(m*n)/D D 0 0 0 0 0 0 0 0 0;
       0 0 0 l m n 0 0 0 0 0 0;
       0 0 0 -m/D l/D 0 0 0 0 0 0;
       0 0 0 -(l*n)/D -(m*n)/D D 0 0 0 0 0 0;
       0 0 0 0 0 0 l m n 0 0 0;
       0 0 0 0 0 0 -m/D l/D 0 0 0 0;
       0 0 0 0 0 0 -(l*n)/D -(m*n)/D D 0 0 0;
       0 0 0 0 0 0 0 0 0 l m n;
       0 0 0 0 0 0 0 0 0 -m/D l/D 0;
       0 0 0 0 0 0 0 0 0 -(l*n)/D -(m*n)/D D];

K_E2 = T_E2'*k_E2*T_E2;

out_E2 = K_E2(7:12,7:12);
```

Substituting Values for Element 3.

```
E = 30*10^6;
G = 11.5*10^6;
A = pi;
L = 32.016;
J = pi/2;
I = 1485.250713;

l = -1250/2001;
m = 3125/4002;
n = 0;
D = 1;

k_E3= [(A*E)/L 0 0 0 0 0 -(A*E)/L 0 0 0 0 0;
      %u1
      0 (12*E*I)/L^3 0 0 0 (6*E*I)/L^2 0 -(12*E*I)/L^3 0 0 0 (6*E*I)/
L^2;   %v1
      0 0 (12*E*I)/L^3 0 -(6*E*I)/L^2 0 0 0 -(12*E*I)/L^3 0 -(6*E*I)/
L^2 0; %w1
      0 0 0 G*J/L 0 0 0 0 0 -G*J/L 0 0;
      %phi_1x
```

```
      0 0 -(6*E*I)/L^2 0 (4*E*I)/L 0 0 0 (6*E*I)/L^2 0 (2*E*I)/L 0;
      %phi_1y
      0 (6*E*I)/L^2 0 0 0 (4*E*I)/L 0 -(6*E*I)/L^2 0 0 0 (2*E*I)/L;
      %phi_1z
      -(A*E)/L 0 0 0 0 0 (A*E)/L 0 0 0 0 0;
      %u2
      0 -(12*E*I)/L^3 0 0 0 -(6*E*I)/L^2 0 (12*E*I)/L^3 0 0 0 -
(6*E*I)/L^2; %v2
      0 0 -(12*E*I)/L^3 0 (6*E*I)/L^2 0 0 0 (12*E*I)/L^3 0 (6*E*I)/L^2
 0;   %w2
      0 0 0 -G*J/L 0 0 0 0 0 G*J/L 0 0;
      %phi_2x
      0 0 (6*E*I)/L^2 0 (2*E*I)/L 0 0 0 (6*E*I)/L^2 0 (4*E*I)/L 0;
      %phi_2y
      0 (6*E*I)/L^2 0 0 0 (2*E*I)/L 0 -(6*E*I)/L^2 0 0 0 (4*E*I)/L];
      %phi_2z

T_E3 = [l m n 0 0 0 0 0 0 0 0 0;
       -m/D l/D 0 0 0 0 0 0 0 0 0;
       -(l*n)/D -(m*n)/D D 0 0 0 0 0 0 0 0;
       0 0 0 l m n 0 0 0 0 0 0;
       0 0 0 -m/D l/D 0 0 0 0 0 0;
       0 0 0 -(l*n)/D -(m*n)/D D 0 0 0 0 0;
       0 0 0 0 0 0 l m n 0 0 0;
       0 0 0 0 0 0 -m/D l/D 0 0 0;
       0 0 0 0 0 0 -(l*n)/D -(m*n)/D D 0 0;
       0 0 0 0 0 0 0 0 0 l m n;
       0 0 0 0 0 0 0 0 0 -m/D l/D 0;
       0 0 0 0 0 0 0 0 0 -(l*n)/D -(m*n)/D D];

K_E3 = T_E3'*k_E3*T_E3;

out_E3 = K_E3(7:12,7:12);
```

Substituting Values for Element 4.

```
E = 30*10^6;
G = 11.5*10^6;
A = pi;
L = 32.016;
J = pi/2;
I = 1485.250713;

l = 625/2001;
m = 3125/4002;
n = 0.541;
D = 0.841;

k_E4 = [(A*E)/L 0 0 0 0 0 -(A*E)/L 0 0 0 0 0;
      %u1
      0 (12*E*I)/L^3 0 0 0 (6*E*I)/L^2 0 -(12*E*I)/L^3 0 0 0 (6*E*I)/
L^2;   %v1
```

```
      0 0 (12*E*I)/L^3 0 -(6*E*I)/L^2 0 0 0 -(12*E*I)/L^3 0 -(6*E*I)/
L^2 0; %w1
      0 0 0 G*J/L 0 0 0 0 0 -G*J/L 0 0;
      %phi_1x
      0 0 -(6*E*I)/L^2 0 (4*E*I)/L 0 0 0 (6*E*I)/L^2 0 (2*E*I)/L 0;
      %phi_1y
      0 (6*E*I)/L^2 0 0 0 (4*E*I)/L 0 -(6*E*I)/L^2 0 0 0 (2*E*I)/L;
      %phi_1z
      -(A*E)/L 0 0 0 0 0 (A*E)/L 0 0 0 0 0;
      %u2
      0 -(12*E*I)/L^3 0 0 0 -(6*E*I)/L^2 0 (12*E*I)/L^3 0 0 0 -
(6*E*I)/L^2; %v2
      0 0 -(12*E*I)/L^3 0 (6*E*I)/L^2 0 0 0 (12*E*I)/L^3 0 (6*E*I)/L^2
 0;   %w2
      0 0 0 -G*J/L 0 0 0 0 0 G*J/L 0 0;
      %phi_2x
      0 0 (6*E*I)/L^2 0 (2*E*I)/L 0 0 0 (6*E*I)/L^2 0 (4*E*I)/L 0;
      %phi_2y
      0 (6*E*I)/L^2 0 0 0 (2*E*I)/L 0 -(6*E*I)/L^2 0 0 0 (4*E*I)/L];
      %phi_2z

T_E4 = [l m n 0 0 0 0 0 0 0 0 0;
       -m/D l/D 0 0 0 0 0 0 0 0 0;
       -(l*n)/D -(m*n)/D D 0 0 0 0 0 0 0 0;
       0 0 0 l m n 0 0 0 0 0;
       0 0 0 -m/D l/D 0 0 0 0 0;
       0 0 0 -(l*n)/D -(m*n)/D D 0 0 0 0 0;
       0 0 0 0 0 0 l m n 0 0 0;
       0 0 0 0 0 0 -m/D l/D 0 0 0;
       0 0 0 0 0 0 -(l*n)/D -(m*n)/D D 0 0 0;
       0 0 0 0 0 0 0 0 0 l m n;
       0 0 0 0 0 0 0 0 0 -m/D l/D 0;
       0 0 0 0 0 0 0 0 0 -(l*n)/D -(m*n)/D D];

K_E4 = T_E4'*k_E4*T_E4;

out_E4 = K_E4(7:12,7:12);
```

Adding all OUT matrices to get Global Non-Zero K.

```
K_G = zeros(30, 30);

K_G(1:6, 1:6) = K_G(1:6, 1:6) + K_E1(1:6, 1:6);
K_G(25:30, 1:6) = K_G(25:30, 1:6) + K_E1(7:12, 1:6);
K_G(1:6, 25:30) = K_G(1:6, 25:30) + K_E1(1:6, 7:12);

K_G(7:12, 7:12) = K_G(7:12, 7:12) + K_E2(1:6, 1:6);
K_G(25:30, 7:12) = K_G(25:30, 7:12) + K_E2(7:12, 1:6);
K_G(7:12, 25:30) = K_G(7:12, 25:30) + K_E2(1:6, 7:12);

K_G(13:18, 13:18) = K_G(13:18, 13:18) + K_E3(1:6, 1:6);
```

```
K_G(25:30, 13:18) = K_G(25:30, 13:18) + K_E3(7:12, 1:6);
K_G(13:18, 25:30) = K_G(13:18, 25:30) + K_E3(1:6, 7:12);

K_G(19:24, 19:24) = K_G(19:24, 19:24) + K_E4(1:6, 1:6);
K_G(25:30, 19:24) = K_G(25:30, 19:24) + K_E4(7:12, 1:6);
K_G(19:24, 25:30) = K_G(19:24, 25:30) + K_E4(1:6, 7:12);

K_G(25:30, 25:30) = K_G(25:30, 25:30) + K_E1(7:12, 7:12) + K_E2(7:12,
 7:12) + K_E3(7:12, 7:12) + K_E4(7:12, 7:12);

K_G
final_K = vpa(out_E1 + out_E2 + out_E3 + out_E4)

% Adding Boundary Conditions and Forces and Solving the System.
F = [0;-6000;0;0;0;0];
dis = linsolve(final_K, F)


K_G =

   1.0e+10 *

  Columns 1 through 7

    0.0107         0         0         0         0   -0.1336         0
         0    0.0015         0         0         0         0         0
         0         0    0.0107    0.1336         0         0         0
         0         0    0.1336    2.2268         0         0         0
         0         0         0         0    0.0012         0         0
   -0.1336         0         0         0         0    2.2268         0
         0         0         0         0         0         0    0.0015
         0         0         0         0         0         0   -0.0003
         0         0         0         0         0         0    0.0002
         0         0         0         0         0         0    0.0000
         0         0         0         0         0         0   -0.0141
         0         0         0         0         0         0   -0.0204
         0         0         0         0         0         0         0
         0         0         0         0         0         0         0
         0         0         0         0         0         0         0
         0         0         0         0         0         0         0
         0         0         0         0         0         0         0
         0         0         0         0         0         0         0
         0         0         0         0         0         0         0
         0         0         0         0         0         0         0
         0         0         0         0         0         0         0
         0         0         0         0         0         0         0
         0         0         0         0         0         0         0
   -0.0107         0         0         0         0    0.1336   -0.0015
         0   -0.0015         0         0         0         0    0.0003
         0         0   -0.0107   -0.1336         0         0   -0.0002
         0         0   -0.1336    1.1134         0         0   -0.0097
         0         0         0         0   -0.0012         0   -0.0102
   -0.1336         0         0         0         0    1.1134   -0.0204
```

Columns 8 through 14

0	0	0	0	0	0	0
0	0	0	0	0	0	0
0	0	0	0	0	0	0
0	0	0	0	0	0	0
0	0	0	0	0	0	0
0	0	0	0	0	0	0
-0.0003	0.0002	-0.0000	-0.0141	-0.0204	0	0
0.0008	0.0006	0.0141	-0.0000	0.0081	0	0
0.0006	0.0012	0.0204	-0.0081	0	0	0
0.0141	0.0204	0.5024	-0.1358	0.0941	0	0
0.0000	-0.0081	-0.1358	0.2173	0.2351	0	0
0.0081	0	0.0941	0.2351	0.3938	0	0
0	0	0	0	0	0.0011	0.0007
0	0	0	0	0	0.0007	0.0008
0	0	0	0	0	0	0
0	0	0	0	0	0	0
0	0	0	0	0	0	0
0	0	0	0	0	-0.0204	-0.0163
0	0	0	0	0	0	0
0	0	0	0	0	0	0
0	0	0	0	0	0	0
0	0	0	0	0	0	0
0	0	0	0	0	0	0
0	0	0	0	0	0	0
0.0003	-0.0002	0.0000	0.0141	0.0204	-0.0011	-0.0007
-0.0008	-0.0006	-0.0141	0.0000	-0.0081	-0.0007	-0.0008
-0.0006	-0.0012	-0.0204	0.0081	0	0	0
-0.0102	-0.0204	0.2512	-0.0679	0.0470	0	0
0.0097	0.0081	-0.0679	0.1086	0.1176	0	0
0.0081	0	0.0470	0.1176	0.1969	-0.0204	-0.0163

Columns 15 through 21

0	0	0	0	0	0	0
0	0	0	0	0	0	0
0	0	0	0	0	0	0
0	0	0	0	0	0	0
0	0	0	0	0	0	0
0	0	0	0	0	0	0
0	0	0	0	0	0	0
0	0	0	0	0	0	0
0	0	0	0	0	0	0
0	0	0	0	0	0	0
0	0	0	0	0	0	0
0	0	0	0	0	0	0
0	0	0	-0.0204	0	0	0
0	0	0	-0.0163	0	0	0
0.0016	0.0204	0.0163	0	0	0	0
0.0204	0.3395	0.2715	0	0	0	0
0.0163	0.2715	0.2173	0	0	0	0
0	0	0	0.5567	0	0	0

```
         0         0         0         0    0.0015   -0.0003   -0.0002
         0         0         0         0   -0.0003    0.0008   -0.0006
         0         0         0         0   -0.0002   -0.0006    0.0012
         0         0         0         0   -0.0000   -0.0141    0.0204
         0         0         0         0    0.0141   -0.0000   -0.0081
         0         0         0         0   -0.0204    0.0081         0
         0         0         0    0.0204   -0.0015    0.0003    0.0002
         0         0         0    0.0163    0.0003   -0.0008    0.0006
   -0.0016   -0.0204   -0.0163         0    0.0002    0.0006   -0.0012
   -0.0204    0.1697    0.1358         0    0.0097    0.0102   -0.0204
   -0.0163    0.1358    0.1086         0    0.0102   -0.0097    0.0081
         0         0         0    0.2783   -0.0204    0.0081         0

Columns 22 through 28

         0         0         0   -0.0107         0         0         0
         0         0         0         0   -0.0015         0         0
         0         0         0         0         0   -0.0107    0.1336
         0         0         0         0         0   -0.1336    1.1134
         0         0         0         0         0         0         0
         0         0         0    0.1336         0         0         0
         0         0         0   -0.0015    0.0003   -0.0002   -0.0000
         0         0         0    0.0003   -0.0008   -0.0006    0.0141
         0         0         0   -0.0002   -0.0006   -0.0012    0.0204
         0         0         0   -0.0000   -0.0141   -0.0204    0.2512
         0         0         0    0.0141   -0.0000    0.0081   -0.0679
         0         0         0    0.0204   -0.0081         0    0.0470
         0         0         0   -0.0011   -0.0007         0         0
         0         0         0   -0.0007   -0.0008         0         0
         0         0         0         0         0   -0.0016    0.0204
         0         0         0         0         0   -0.0204    0.1697
         0         0         0         0         0   -0.0163    0.1358
         0         0         0    0.0204    0.0163         0         0
    0.0000    0.0141   -0.0204   -0.0015    0.0003    0.0002    0.0000
   -0.0141    0.0000    0.0081    0.0003   -0.0008    0.0006   -0.0141
    0.0204   -0.0081         0    0.0002    0.0006   -0.0012    0.0204
    0.5024   -0.1358   -0.0941    0.0000    0.0141   -0.0204    0.2512
   -0.1358    0.2173   -0.2351   -0.0141    0.0000    0.0081   -0.0679
   -0.0941   -0.2351    0.3938    0.0204   -0.0081         0   -0.0470
   -0.0000   -0.0141    0.0204    0.0148   -0.0000         0         0
    0.0141   -0.0000   -0.0081   -0.0000    0.0040         0         0
   -0.0204    0.0081         0         0         0    0.0148   -0.1947
    0.2512   -0.0679   -0.0470         0         0   -0.1947    3.5710
   -0.0679    0.1086   -0.1176         0         0   -0.0000   -0.0000
   -0.0470   -0.1176    0.1969    0.1947         0         0         0

Columns 29 through 30

         0   -0.1336
         0         0
         0         0
         0         0
   -0.0012         0
         0    1.1134
```

```
   -0.0141   -0.0204
   -0.0000    0.0081
   -0.0081         0
   -0.0679    0.0470
    0.1086    0.1176
    0.1176    0.1969
         0   -0.0204
         0   -0.0163
    0.0163         0
    0.1358         0
    0.1086         0
         0    0.2783
    0.0141   -0.0204
    0.0000    0.0081
   -0.0081         0
   -0.0679   -0.0470
    0.1086   -0.1176
   -0.1176    0.1969
         0    0.1947
         0    0.0000
         0         0
   -0.0000         0
    0.6530         0
         0    3.5710


final_K =

[ 147950200.58543461561203002929688,
 -427.00063728541135787963867 1875,
 0,                                  0,                                  0,
 1947048298.469356536865234375]
[-427.00063728634268045425415039062,
 39539339.383599624037742614746094,
 0,                                  0,                                  0,
 0.00000002980232238769531 25]
[                                   0,
 0, 147948494.3804978728294372558593 8, -1947048298.469356536865234375,
                                    0,                                  0]
[                                   0,
 0,    -1947048298.469356536865234375,    35710244717.155731201171875,
    -145895.33684825897216796875,                                  0]
[                                   0,
 0,      -0.00000002980232238769531 25,  -145895.33684873580932617187 5,
 6529996236.79280185699462890625,                                  0]
[     1947048298.469356536865234375,
 0,                                   0,                                  0,
                                  0, 35709651699.195350646972656 25]


dis =

 -0.00000000155057758739718465690503492050 32
      -0.00015174760363221484092177258132456
```

```
                                                    0
                                                    0
                                                    0
0.000000000084544354524030177615821728418017
```

Solving for Element 1.

```
dis_E1 = [0;0;0;0;0;0;dis];
f_E1 = k_E1*T_E1*dis_E1

% Solving for Element 2.
dis_E2 = [0;0;0;0;0;0;dis];
f_E2 = k_E2*T_E2*dis_E2

% Solving for Element 3.
dis_E3 = [0;0;0;0;0;0;dis];
f_E3 = k_E3*T_E3*dis_E3

% Solving for Element 4.
dis_E4 = [0;0;0;0;0;0;dis];
f_E4 = k_E4*T_E4*dis_E4

% Solving fot Global Forces.
dis_G = [0;0;0;0;0;0;0;0;0;0;0;0;0;0;0;0;0;0;0;0;0;0;0;0;0;0;0;0;dis];
F_G = K_G*dis_G


f_E1 =

 2288.2999524999453448369230611909
-0.052776876609536820655106143960 5
                                  0
                                  0
                                  0
-1.130362615706124667392631061151 5
-2288.2999524999453448369230611909
 0.052776876609536820655106143960 5
                                  0
                                  0
                                  0
-0.189059299532296514646490468421 8


f_E2 =

     348.81938341473133435337550660619
     918.24274887361076709171650789436
     1241.9350378119953804486752477645
 0.000025806703014309388690519626569 12
    -19880.896085294417323134385579269
     14699.130969693694951730851005965
    -348.81938341473133435337550660619
```

```
    -918.24274887361076709171650789436
    -1241.93503781199538044867524776 45
-0.00002580670301430938869051962656912
    -19880.89608529441732313438557926 9
     14699.32887824381839075196287595 7


f_E3 =

  348.81510629171108732586766985 15
-1544.49024265762554187624070336 05
                                   0
                                   0
                                   0
-24724.31746709711043550355515765 5
 -348.81510629171108732586766985 15
 1544.49024265762554187624070336 05
                                   0
                                   0
                                   0
-24724.08214182942501456531732536 4


f_E4 =

     348.81938341473133435337550660619
     918.24274887361076709171650789436
    -1241.93503781199538044867524776 45
-0.00002580670301430938869051962656912
     19880.89608529441732313438557926 9
     14699.13096969369495173085100596 5
    -348.81938341473133435337550660619
    -918.24274887361076709171650789436
     1241.93503781199538044867524776 45
 0.00002580670301430938869051962656912
     19880.89608529441732313438557926 9
     14699.32887824381839075196287595 7


F_G =

     0.05277687660953682065510614396 05
     2288.29995249994534483692306119 09
                                      0
                                      0
                                      0
    -1.13036261570612466739263106115 15
    -494.09113638630618142523581713692
     1237.25022192523224524289507492 46
     855.75608037251854391058145682658
     21412.62531989941848858760166223 1
   -0.11936456158619352507895132238694
      12361.96913155097218191264119731
     988.12949589600282603559287977322
```

```
      1237.19960364959044732922460192 7
                                      0
                                      0
                                      0
    -24724.31746709711043550355515765 5
    -494.09113638630618142523581713692
     1237.25022192523224524289507492 46
    -855.75608037251854391058145682658
    -21412.62531989941848858760166223 1
    0.11936456158619352507895132238694
      12361.96913155097218191264119731
-4.59177480789956057800287709852 44e-41
                                -6000.0
                                      0
                                      0
                                      0
  7.34683969263929692480460335763 9e-40
```

Published with MATLAB® R2021a